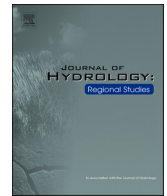




ELSEVIER

Contents lists available at [ScienceDirect](https://www.sciencedirect.com)

Journal of Hydrology: Regional Studies

journal homepage: www.elsevier.com/locate/ejrh

Runoff and sediment loads in the Tijuana River: Dam effects, extreme events, and change during urbanization

Trent Biggs^{a,*}, Adam Zeigler^a, Kristine T. Taniguchi-Quan^b

^a Department of Geography, San Diego State University, San Diego, CA, USA

^b Southern California Coastal Water Research Project, 3535 Harbor Blvd Suite 110, Costa Mesa, CA 92626, USA

ARTICLE INFO

Keywords:

Suspended sediment
Rainfall-runoff
Extreme events
Semi-arid
Uncertainty
Bootstrapping

ABSTRACT

Study region: Tijuana River watershed on the US-Mexico border, where urbanization, estuarine sedimentation, and beach erosion incentivize quantification of runoff and suspended sediment loads (SSL) and concentrations (SSC).

Study focus: Rainfall, runoff and SSL were quantified for 2001–2019 (storm-wise) and 1962–2019 (annual) using sediment rating curves and bootstrapping to quantify uncertainty.

New hydrological insights: Annual runoff increased for a given rainfall depth following channelization and the start of imported water in 1978–79, and during urbanization over 1980–2019. SSC for a given runoff fell between 1970 s and 2000 s, but annual SSL increased severalfold due to higher annual runoff. Half the SSL over 2001–2019 occurred during nine storms. Nearly half (48 %) of annual SSL occurred in the six wettest years over 1962–2019, though years with recurrence interval 2–10 years accounted for 50 %. Neglecting the impact of dams on the SSL-rainfall relationship during extreme wet years over-estimated annual SSL by a factor of 7 and by up to 30x for the wettest year. Long-term mean suspended sediment yield ($119 \text{ tons km}^{-2} \text{ yr}^{-1}$) is similar to other southern California watersheds but much lower than observed ($5000 \text{ tons km}^{-2} \text{ yr}^{-1}$) in a small watershed that also drains to the Tijuana estuary. Accumulation of sediment in the estuary may be driven by undammed side canyons, and by low runoff that cannot transport sediment to the coast.

1. Introduction

Sediment loading to the coast is critical for both ecosystems and coastal geomorphology. Globally (Mentaschi et al., 2018; Walling, 2012) and in California (Slagel and Griggs, 2008; Willis and Griggs, 2003) dam construction has decreased sediment loads to the coast, threatening wetland and beach stability. In southern California, post-dam sediment loads are less than 50 % of pre-dam loads, resulting in beach erosion and expensive beach nourishment activities (Slagel and Griggs, 2008). By contrast, land use change, including the construction phase of urbanization (Wolman, 1967), road construction (Tarolli and Sofia, 2016), mining (Messina and Biggs, 2016),

Abbreviations: A_{lower} , Area of the lower watershed, km^2 ; A_{total} , Area of the whole watershed, km^2 ; bcf, Bias correction factor; Q_{ann} , Annual runoff, MCM; $Q_{\text{ann,lower}}$, Annual runoff from the lower watershed only, MCM; $Q_{\text{ann,total}}$, Annual runoff from the total watershed, MCM; Q_{pk} , Peak runoff for a given storm, $\text{m}^3 \text{ s}^{-1}$; SSC, Suspended sediment concentration, mg L^{-1} ; SSL, Suspended sediment load, ton y^{-1} or Mt y^{-1} ; SSL_{ann} , Annual suspended sediment load, ton y^{-1} or Mt y^{-1} .

* Correspondence to: Department of Geography, San Diego State University, 5555 Canyon Crest Drive, San Diego, CA 92812, USA.

E-mail address: tbiggs@sdsu.edu (T. Biggs).

<https://doi.org/10.1016/j.ejrh.2022.101162>

Received 22 February 2022; Received in revised form 10 June 2022; Accepted 28 June 2022

Available online 18 July 2022

2214-5818/© 2022 The Authors. Published by Elsevier B.V. This is an open access article under the CC BY license (<http://creativecommons.org/licenses/by/4.0/>).

and agriculture (Dedkov and Mozzerhin, 1996) generally increase sediment loads, particularly from small watersheds, though some urban surfaces may generate less sediment than undisturbed areas due to pavement and revegetation (Wolman, 1967). Other activities, including channelization (Brown, 1988; Simon, 1989) and importing water for human use (Manago and Hogue, 2017), may also increase runoff and change sediment loads. Increased sediment loads can increase sedimentation in coastal wetlands, converting them to upland habitat and triggering costly management interventions (Chapman et al., 2014; Fennessey and Jarrett, 1994).

In southern California and along the US-Mexico border, all four human activities (dams, channelization, water imports and land use change) occur. Parts of the Tijuana River Estuary in southern San Diego County, which receives loads from the cross-border Tijuana River, have experienced high sedimentation rates attributed in part to rapid urbanization (Weis et al., 2001), with consequent impacts on the estuarine ecosystem (Zedler and West, 2008) and tidal channels (Wallace et al., 2005). Rapid urbanization in Tijuana has increased sediment loads above pre-disturbance levels in some locations, where bare soil with high erosion rates can persist for decades (Biggs et al., 2010) and where channel erosion rates can be many times the natural background rate (Taniguchi et al., 2018). However, much of Tijuana has high impervious surface coverage and channelization, which can reduce sediment loads below the natural background (Wolman, 1967), and the municipal government has installed dozens of sedimentation basins in Tijuana to control sediment loads. Several large dams on the Tijuana River and its major tributaries have also reduced the active contributing area of the watershed by 70 %, reducing total runoff and sediment loads by approximately 50 % compared with pre-development conditions, resulting in beach erosion in both the United States and Mexico (Inman and Masters, 1991; Willis and Griggs, 2003). At the same time, smaller canyons (drainage areas $\sim 10 \text{ km}^2$) on erodible sediments with no dams contribute high sediment loads in the southern part of the estuary due to unregulated urbanization on steep hillslopes (Biggs et al., 2018; Gudino-Elizondo et al., 2019) and high rates of stream channel erosion (Taniguchi et al., 2018). The combined impacts of urbanization and dams on the runoff and suspended sediment load (SSL) of the Tijuana River system remain to be determined, including comparisons before (1960–1970 s) and after the large-scale urbanization. The need for updated SSL estimates and change over time is especially critical as government agencies develop plans to mitigate cross-border flows of sewage and sediment.

SSL also varies over time due to climate variability and extreme events. Most of the long-term SSL to coastal California over 1944–1995 was delivered in a few wet years (Inman and Jenkins, 1999), and calculations of long-term SSL must account for the frequency distribution of SSL, especially extreme events (Li et al., 2020). The relationship between rainfall, runoff and SSL may change for large events that trigger releases from dams, since water released from dams typically has lower sediment concentrations than the water entering the dam. However, monitoring and measurement of SSL may be limited to relatively small events, where there may not be overflow from large dams. In California, reservoirs trap 84 % of the SSL entering them (Willis and Griggs, 2003), so extrapolation of sediment rating curves developed using data from small events to extreme events may significantly overestimate SSL.

In this study, data on SSC from historical (1973–1979; 2002–2014) and recent (2019–2021) periods are compiled and combined with long time series of runoff (Q) and rainfall (P) to estimate the relationship between P, Q and SSL for the Tijuana River. The Q-P relationship is tested for change over time, and the SSC-Q and SSL-Q relationships observed in 2001–2021 are compared with data from the 1970 s. The impact of dams on calculations of SSL during wet years receives special attention. We aim to answer: What is the relationship between storm size and sediment loads? What storm sizes and return intervals account for most of the sediment load on decadal timescales? What is the impact of different assumptions about sediment retention by dams on SSL calculations? Have the annual Q-P relationship and sediment rating curves (SSL-Q) changed from the 1970–2010 s? Finally, how does SSL in the Tijuana River compare with loads from smaller watersheds that drain to the Tijuana estuary, and in other watersheds in California? The major

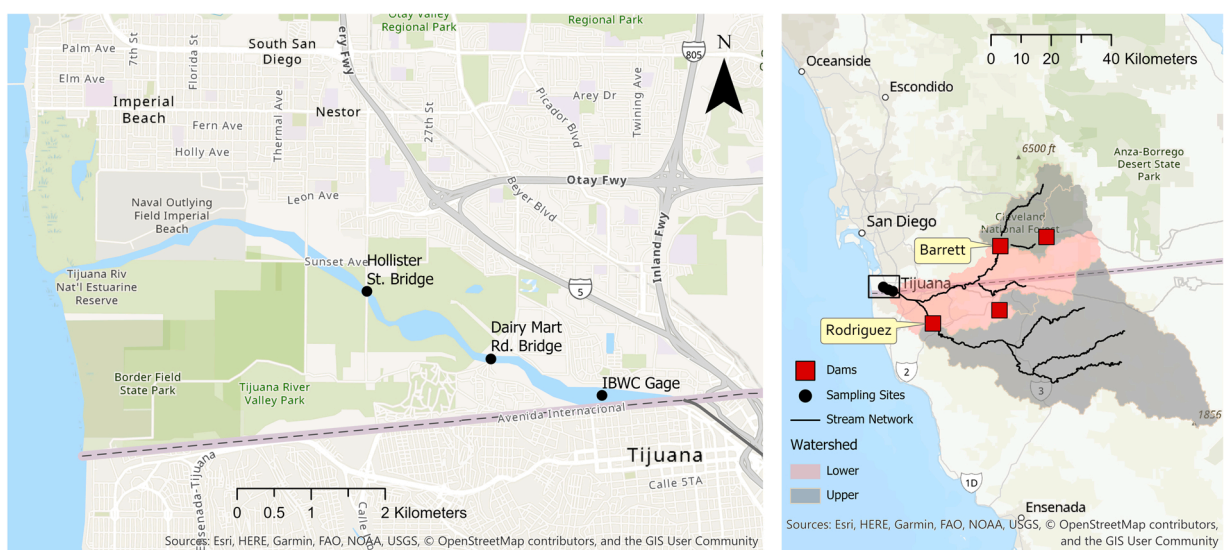


Fig. 1. Map of sampling locations (left) and the Tijuana River watershed (right), showing the areas upstream (Upper) and downstream (Lower) of two major dams (Barrett and Rodriguez).

contributions of the paper are to 1) quantify decadal means, variability and frequency in runoff and SSL; 2) quantify uncertainty in SSL caused by dams and by scatter in the Q-SSL relationship and 3) test for changes in runoff and SSL in a rapidly urbanizing section of the US-Mexico border region.

2. Study area

The Tijuana River watershed (TRW) drains a total of 4483 km², with approximately 27 % of the drainage area in the United States and 73 % in Mexico (International Boundary and Water Commission, 2005) (Fig. 1). The central and eastern parts of the TRW are on the Peninsular range batholith, and the western part is on marine and fluvial deposits of conglomerate, sandstone and siltstone (Brownlie and Taylor, 1981). TRW has two large dams: Barrett dam was built in 1922, has a total capacity of 42.9 MCM (City of San Diego, 2021) and receives runoff from the United States portion of the watershed; the Rodriguez dam was completed in 1936 and has a capacity of 94.0 MCM at the spillway crest (International Boundary and Water Commission, 1966). The drainage area at Barrett Dam is 635 km² (14 % of the TRW) (City of San Diego, 2021), and at Rodriguez dam is 2251 km² (57 % of the TRW) (URS Corporation, 2012a). The remaining lower watershed ($A_{\text{lower}}=1138 \text{ km}^2$, 29 %), which is the active contributing watershed in all but very wet years, straddles the US-Mexico border and includes the urban areas of Tijuana and Tecate. The active contributing area in the US is mostly undeveloped open space. A third dam, El Carrizo, was added in 1978 to impound water imported from the Colorado River. The watershed draining to the El Carrizo dam is very small (2.6 % of the watershed) and the dam has no overflow (URS Corporation, 2012b), so we do not include it in the analysis of runoff and SSL.

Urbanization has expanded rapidly in Tijuana due to economic opportunity and consequent immigration (Acosta, 2009). Much of the urbanization is unregulated, with extensive and chronic soil exposure (Biggs et al., 2010), unpaved roads that generate ephemeral gullies (Gudino-Elizondo et al., 2018), and extreme channel erosion (Taniguchi et al., 2018). To mitigate the sediment loads, sedimentation basins have been constructed both in the United States and Mexico. Excess sedimentation has buried salt marsh vegetation in the Tijuana Estuary in the United States (Weis et al., 2001; Zedler and West, 2008). Wetland loss has been most severe at the outlets of three small watersheds that drain directly to the southern part of the estuary (Safran et al., 2017). The lower reach of Tijuana River was channelized in early 1979, in part in response to previous flooding. A total of 4 km of channel was lined with concrete from the border upstream, and an additional 2 km lined with rock downstream of the border (International Boundary and Water Commission, 2021). Tijuana started importing water from the Colorado River in 1978 (URS Corporation, 2012b), increasing to 76.7 MCM y⁻¹ in 2000 and 101.3 MCM y⁻¹ in 2008 (Cohen et al., 2011).

3. Materials and methods

We compiled data on rainfall, runoff (Section 3.1), and SSC (Section 3.2) for the Tijuana River where it enters the Tijuana Estuary. SSC data included both historical data and our own samples. We then developed a relationship between storm-wise peak runoff (Q_{pk}) and storm-wise mean SSC for 2002–2021 (Section 3.3). Storm-wise SSL was then estimated for all storms for the water years that had 10-minute runoff data (2001–2020) and aggregated to annual values of SSL. The annual SSL values for 2001–2020 were used to develop an annual SSL-Q relationship, which was then used to estimate annual SSL for all years over 1962–2020, including sensitivity analysis of the impact of dams (Section 3.4). Finally, we tested for changes in the Q-P and SSL-Q relationships between 1970 s and 2000 s and compare with other studies (Section 3.5).

3.1. Rainfall and runoff data

Runoff (Q) in the mainstem Tijuana River has been measured by the International Boundary and Water Commission (IBWC) since 1962 upstream of where the river enters the Tijuana Estuary (Fig. 1). Runoff data at ten-minute resolution are available from 2000 to 2020, and daily means from 1962 to 2020 (International Boundary and Water Commission, 2021). Monthly rainfall for both the lower and total watershed (Fig. 1) was calculated for 1962–2020 from the ERA5-Land dataset (Muñoz-Sabater, 2019; Muñoz-Sabater et al., 2021), which has 9 km cell size. Annual rainfall and runoff were aggregated using the Oct-Sept water year.

Data on runoff over the spillway at Barrett Reservoir were obtained from the City of San Diego (R. Morales, personal communication), and historical observations indicated if spillway overflow occurred at the Rodriguez dam (URS corporation, 2012 for 1970–2009 and R. Morales, personal communication, for 2010–2020).

3.2. SSC data

We compiled historical data on SSC of the Tijuana River from a municipal monitoring program (2002–2014) (Weston Solutions, 2015) and from the United States Geological Survey (USGS) (1970 s). We also collected our own water samples in 2019–2021 and analyzed them for suspended sediment concentrations (SSC). The historical data were reported as either total suspended solids (TSS) (2002–2014) or SSC (1970 s), and the new samples (2019–2021) were analyzed for SSC. TSS and SSC differ in the method of sub-sampling in the laboratory; see S1.0 for details. Following recommendations of Gray et al. (2000), we do not attempt to correct the TSS values to SSC, and assume that the difference between TSS and SSC values is small compared to other uncertainties in the calculation of SSL.

TSS values in stormwater were obtained from an existing report (Weston Solutions, 2015). Composite samples were taken from Hollister Bridge (Fig. 1) for twenty-two storms sampled from January 2002 to March 2014. All samples were volume-weighted

composites, though some samples had more frequent sampling on the rising limb (see S2.0 and Fig. S1). The USGS reported 182 values of SSC from Hollister Bridge over 1970–1978, station 11013500 (United States Geological Survey, 2016, <http://waterdata.usgs.gov/nwis/>, access date 2021-06-21)(Fig. 1). Additional water samples were taken by the authors from the Tijuana River in 2019–2021 at Dairy Mart Road Bridge (DMR, Fig. 1) with a combination of grab samples and an autosampler that took samples once an hour. See S3.1 for details of the water sampling, SSC methods and SSC data.

3.3. Storm metrics and SSC

Traditional sediment rating curves, where instantaneous SSL is modeled as a function of instantaneous runoff, may result in significant error given intra-event hysteresis in SSC (Warrick et al., 2015). Management agencies also often only collect composite samples and report storm-wise mean SSC, complicating the use of instantaneous rating curves. Storm metrics, such as total or peak runoff (Q_{pk}), may provide more accurate predictions of SSC and SSL than instantaneous sediment rating curves (Duvert et al., 2012). In California, Q_{pk} correlates with sediment yield in individual watersheds, but the relationship varies by location (Warrick et al., 2015). We therefore modeled storm-wise mean SSC as a power function of Q_{pk} (Duvert et al., 2012):

$$SSC = bcf_{SSCQ_{pk}} aQ_{pk}^b \quad (1)$$

where a and b are determined through linear regression on the log-transformed values of SSC and Q_{pk} , and $bcf_{SSCQ_{pk}}$ is a bias correction factor (Crawford, 1991) that compensates for the underestimation that occurs when using minimum least-squares on log-transformed variables. The regression parameters were calibrated to the data collected from 2002 to 2021. Outliers were identified using the Tukey fence method and the impact of outliers quantified by comparing regression parameters, annual Q and annual SSL with and without outliers. See S3.2 for details.

In order to calculate annual SSL for the period with 10-minute runoff data (2001–2020), the EcoHydrology package (Fuka et al., 2018) in R (R Core Team, 2021) was used to separate streamflow into stormflow and baseflow. Q_{pk} and total stormflow volume were then calculated for each storm. SSC was estimated for each storm using Eq. (1), and SSL calculated as the product of total volume and SSC. See S3.3 for details. Suspended sediment yield (SSY) was calculated by dividing SSL by the drainage area of the lower watershed (A_{lower} , Fig. 1) since watersheds upstream of dams contributed flows in only a few years.

3.4. Annual SSL and accounting for dams

Sub-daily runoff data were not available for 1962–2000, so we could not use a storm-wise SSC- Q_{pk} relationship (Eq. 1) to estimate annual SSL (SSL_{ann}) for years before 2001. Instead, we estimated SSL_{ann} (tons) for the whole period (1962–2020) from annual Q (Q_{ann} , MCM):

$$SSL_{ann} = bcf_{ann} cQ_{ann}^d \quad (2)$$

where bcf_{ann} is the bias correction factor for annual values, and c and d are regression parameters.

All of the available SSC data were collected during periods with no overflow from the two main dams (Barrett and Rodriguez); sediment retention behind the dams could cause SSC and SSL to be lower than predicted by Eq. (2) during wet periods with spillway overflow. In order to quantify the impact of different assumptions about dam impacts on SSL estimates, we calculated SSL for years with overflow using Eq. 2 given two different values of Q : 1) $Q_{ann,tot}$, which includes overflow and assumes that overflow from the dams does not change the SSL- Q relationship (Eq. 2), and 2) $Q_{ann,lower}$, which excludes overflow and is estimated as:

$$Q_{ann,lower} = bcf_{QP} gP_{ann,lower}^h \quad (3)$$

where bcf_{QP} is the bias correction factor for the Q - P regression, $P_{ann,lower}$ is annual rainfall in the lower watershed, and g and h are regression parameters. SSL_{ann} at the outlet for years with overflow is then calculated from Eq. 2 with $Q_{ann,lower}$ as the predictor, which assumes complete retention of sediment in the reservoirs and no channel erosion downstream of the dams; the channel downstream of Rodriguez dam is channelized with concrete and has limited opportunity for erosion (URS Corporation, 2012a). Note that this sensitivity analysis does not determine the impact of dams per se on long-term sediment load; the SSL- Q relationship (Eq. 2) already includes the impact of dams because the data to calibrate Eq. 1 were collected in the post-dam period. Rather, we quantify the impact of assumptions about dams on SSL calculations for years with overflow.

The combined impact of Q - P and SSL- Q on annual SSL was determined by creating an SSL- P relationship:

$$SSL_{ann} = bcf_{SSLP} mP_{ann,lower}^n \quad (4)$$

where bcf_{SSLP} is the bias correction factor and m and n are regression parameters. This regression assumes that dams retain all sediment that enters the corresponding reservoir.

Errors in SSL estimates can be quantified using standard statistical techniques, which may be less applicable if the data are non-normal, or if multiple types of uncertainty are present. Alternatively, bootstrapping and Monte Carlo methods (Rustomji and Wilkinson, 2008) can be used to estimate uncertainty. We used bootstrapping with replacement to generate 1000 SSC- Q_{pk} data sets, and therefore 1000 estimates of the parameters of the SSC- Q_{pk} relationship (Eq. 1). These parameters were used to estimate ensembles of

1000 values each of 1) SSL_{ann} for 2001–2020, 2) parameters of Eq. 2, and 3) values of SSL_{ann} for each year from 1962 to 2020.

3.5. Change over time and comparisons with other studies

We tested for changes in the annual Q-P relationship before and after the start of imported water (1978) and channelization (1979) both of which occurred within several months of each other so we were unable to separate their effects. We instead refer to pre- and post-1978 periods, where the pre-1978 period includes the 1962–1978 water years. The statistical significance of changes in the coefficients of the power functions (Eqs. 2–4) were tested using linear regression on the log-transformed variables, including pre- or post-1978 as an indicator variable (0 or 1), and an interaction term between the continuous variables (P or Q) and the indicator.

Changes in the annual Q-P relationship during the post-1978 period (1979–2019) were determined using multiple regression with P and year as independent variables. SSL_{ann} (2001–2019) and instantaneous SSC (2019–2021) were compared with historical data from 1970 to 1978, and with the annual and instantaneous sediment rating curves of (Brownlie and Taylor, 1981) (hereafter BT81), which were based on data from 1973 to 1975. The combined impact of changes in the Q-P and SSL-Q relationships were quantified by creating SSL-P relationships in the pre- and post-1978 periods. Q and SSL were calculated for a pre-1978 scenario by applying the Q-P (Eq. 3) and SSL-P (Eq. 4) relationships from the pre-1978 period to the P time series in the post-1978 period (1980–2019).

Other studies on the Tijuana River used methods similar to ours to quantify long-term SSL. BT81 calculated SSL for 1937–1975 using an instantaneous sediment rating curve (SSC-Q) developed from 43 samples taken at Hollister Bridge by the USGS from 1973 to 1975. BT81 then estimated SSL_{ann} from a log-linear regression of SSL_{ann} against Q_{ann} , equivalent to Eq. 2 but with no bias correction factor. The highest runoff with SSC data in the analysis of BT81 was very low ($3.23 \text{ m}^3 \text{ s}^{-1}$) compared with both our largest sampled runoff ($128.4 \text{ m}^3 \text{ s}^{-1}$) and with the peak runoff of all storms from 2001 to 2020. BT81 therefore extrapolated well beyond the observed range of runoff, in part due to low runoff in the pre-1978 conditions, increasing uncertainty about SSL during high runoff and wet years in the 1970 s.

Inman and Jenkins (1999) (hereafter IJ99) updated the period of record of SSL estimates to 1995 using the same annual sediment rating curve as BT81 and streamflow data to 1995. IJ99 did not add any more SSC values or recalculate annual rating curves. In order to compare our SSL values with IJ99, we calculated SSL for the same wet period as IJ99 (1969–1995) using our annual SSL-Q relationship (Eq. 2). We also compare our SSL estimates with values from URS Corporation (2012a), who also estimated annual sediment load of the Tijuana River under undisturbed conditions using annual runoff and an empirical equation calibrated to sedimentation rates for reservoirs across the conterminous United States.

4. Results

4.1. SSC results: 2019–2021

Seven storms were sampled at Dairy Mart Road in 2019–2021, and sixty-two samples were analyzed for SSC (Table S1). Data from one storm were omitted; see S4.0 for details, including SSC data and sampled hydrographs (Figs. S2-S8 and Tables S2-S8). The maximum runoff with a water sample during the 2019–2021 period ($128.4 \text{ m}^3 \text{ s}^{-1}$) was close to the largest Q_{pk} of storms sampled over

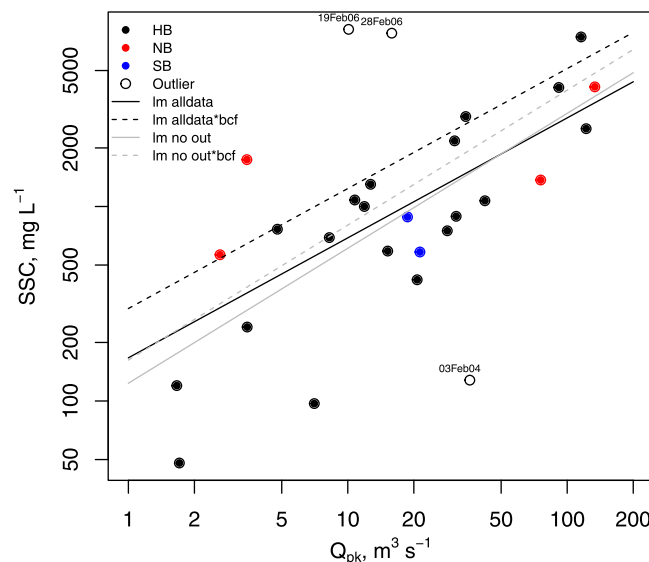


Fig. 2. Peak Discharge (Q_{pk}) vs event mean SSC in the Tijuana River. Samples were taken at Hollister St. Bridge (HB, 2002–2014), or at Dairy Mart Road (DMR) North Branch (NB) or DMR-South Branch (SB) (2019–2021). lm indicates linear models with all data (lm alldata) and without Tukey outliers (lm no out). The dotted lines are the linear regression lines times the bias correction factor (bcf).

2002–2014 ($133.6 \text{ m}^3 \text{ s}^{-1}$). Instantaneous SSC values over 2019–2021 ranged from 95 mg L^{-1} during pre-storm conditions to 5480 mg L^{-1} at the largest sampled runoff.

4.2. Storm-wise sediment rating curves

Storm-wise mean SSC increased linearly with event peak runoff (Q_{pk}) in log-log space (years 2001–2014 and 2019–2021) (Fig. 2). The Tukey (1977) method identified three outliers. The SSC- Q_{pk} regression excluding outliers ($R^2 = 0.61$) was used to estimate SSC for storms with no SSC observations over the 2001–2019 period (See S5.0, Table S9 for details). Storm-wise mean SSC of the storms sampled from 2019 to 2021 fell in the range of the values from 2002 to 2014, with one high mean SSC value at low Q_{pk} ($\sim 4 \text{ m}^3 \text{ s}^{-1}$, Fig. 2). There was no indication of differences in SSC by sampling location (See S4.0 for details).

4.3. Stormflow separation

The stormflow separation algorithm identified 498 storm events over 2001–2020 when using a flow threshold of $1 \text{ m}^3 \text{ s}^{-1}$, a filter parameter (f) of 0.99 and storm separation duration (sephr) of 12 h. Annual Q and SSL were relatively insensitive to the separation parameters (See S6.0, Table S10, Figs. S9–S18). Q_{pk} ranged from 1 to $532 \text{ m}^3 \text{ s}^{-1}$. Many of the storms were small ($< 10 \text{ m}^3 \text{ s}^{-1}$) (Fig. S19), and most Q_{pk} values were smaller than the maximum Q_{pk} in the observed SSC dataset, though 15 storms had Q_{pk} greater than twice the Q_{pk} of the largest storm sampled for SSC. Baseflow was high in 2020 due in part to continual sewage releases (See S6.0) where the Q_{pk} -SSC relationship may not hold, so we excluded the 2020 water year from further analyses.

4.4. Storm-wise and annual suspended sediment load, 2001–2019

SSL_{ann} averaged $0.131 \pm 0.037 \text{ Mt yr}^{-1}$ (SSY = $112.9 \text{ tons km}^{-2} \text{ yr}^{-1}$) over 2001–2019, ranging from 1200 ± 300 tons in 2002 to $587,000 \pm 182,000$ tons in 2017 (Table S11). The twenty largest storms delivered 73 % of the total SSL over the 2001–2019 period, the 10 largest storms delivered 53 %, and the single largest storm 9.5 % (Table S12), demonstrating the importance of large events in the long-term sediment load. However, storms smaller than the 2-year storm accounted for 47 % of the total sediment load, so while a few large storms were important, more numerous smaller storms also accounted for around half of the cumulative SSL. SSL_{ann} (tons) correlated with Q_{ann} (MCM) over 2001–2019 (Fig. 3). Bootstrap regressions provided 1000 estimates of c and d (Fig. 3). The c and d parameters are inversely related, so could not be sampled independently for sensitivity analysis; instead, c and d pairs were selected for bootstrapping. The mean and standard deviation of the regression parameters (Eq. 2) from the bootstrapping were: $bcf_{ann} = 1.1 \pm 0.03$, $c = 260.5 \pm 76.9$ and $d = 1.67 \pm 0.12$.

4.5. Annual Q and Q-P relationships: 1962–2019

The runoff time series has three periods (Table 1, Fig. 4): very low runoff (1962–1978), high runoff with several years of dam overflow (1979–1999), and moderate flow with no dam overflow (2000–2019). Q_{ann} in the 3 wettest years was 5.5, 4.5, and 4.4 times higher than the largest annual flow observed from 2001 to 2019 (US Army Corps of Engineers, 2018). One or both of the two dams

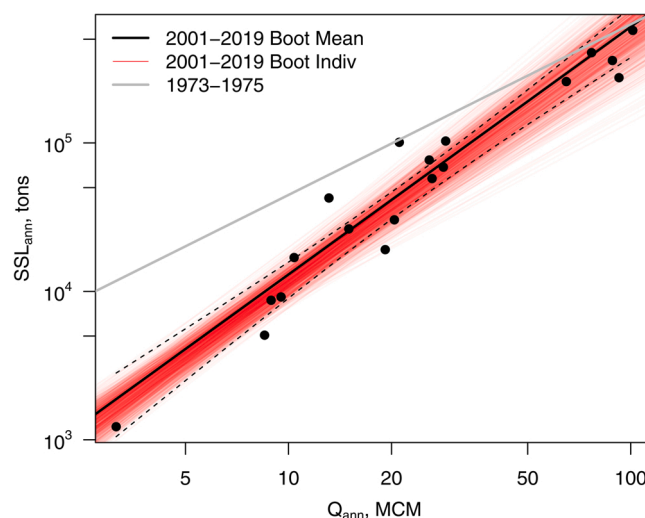


Fig. 3. Annual sediment rating curves (Q_{ann} vs SSL_{ann}) for the Tijuana River for 2001–2019. Each red line (Boot Indiv) is an individual instance of bootstrapping the SSC- Q_{pk} regression and the black line is the mean (Boot Mean). Dotted black lines are the 95 % confidence intervals of the regression. The gray line for 1973–1975 is from Brownlie and Taylor (1981).

Table 1

Annual rainfall (P), runoff (Q) and suspended sediment load (SSL) for individual years with overflow, and long-term means including all years over different periods between 1962 and 2019. P_{ann_lower} and Q_{ann_lower} indicate rainfall and runoff from the lower watershed, and Q_{ann_total} indicates runoff at the IBWC gage, including both the upper and lower watersheds.

WY	P (mm)	Q (MCM)		SSL (Mt)		Ratio ^a
	P_{ann_lower}	Q_{ann_total}	Q_{ann_lower}	$f(Q_{ann_total})^b$	$f(Q_{ann_lower})^c$	
1980	686	732	94	19.32	0.57	33.9
1983	776	591	117	13.35	0.83	16.1
1993	718	599	102	13.67	0.65	21.0
1995	590	217	71	2.38	0.35	6.8
1998	630	89	80	0.52	0.43	1.2
2005	651	88	85	0.51	0.48	1.1
1962–2019	367	58	28	0.92	0.13	7.1
1962–1978	334	6	7	0.03	0.04	0.8
1979–1999	436	124	40	2.39	0.19	12.6
2000–2019	323	33	33	1.30	0.12	10.8

^a . Ratio of SSL calculated using Q_{ann_total} to SSL calculated using Q_{ann_lower} .

^b . SSL calculated using Q_{ann_total} in Eq. (2). Assumes no impact of dams on the SSL_{ann} - Q_{ann} relationship.

^c . SSL calculated using Q_{ann_lower} in Eq. (2). Assumes complete retention of sediment behind dams in years with overflow.

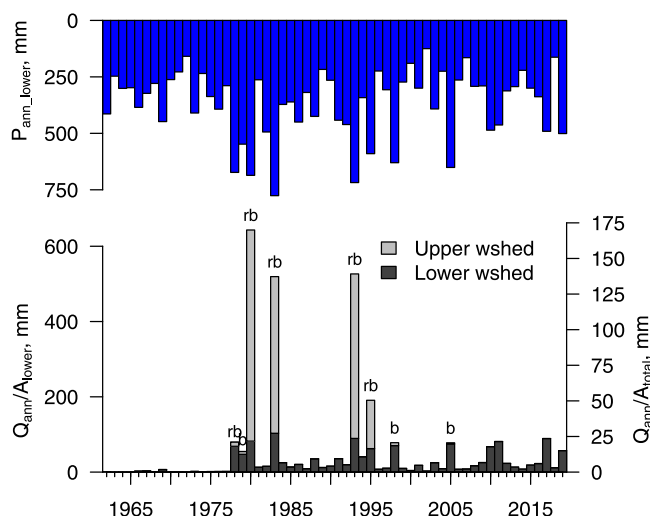


Fig. 4. Time series of observed annual runoff (Q_{ann}) and annual rainfall in the lower watershed (P_{ann_lower}) for the Tijuana River at the IBWC gage (1962–2019). Volumetric runoff was normalized by either the lower watershed area only (A_{lower} , y-axis lhs) or whole watershed (A_{total} , y-axis rhs). Letters above the bars indicate years when Rodriguez (r), Barrett (b) or both (rb) reservoirs had overflow (spillway runoff). Runoff from the lower watershed was taken directly from measurements at the IBWC gage for years with no overflow, and from the Q-P relationship for the lower watershed for years with overflow (Eq. 3).

overflowed in 8 years (14 % of all years) between 1962 and 2019 (Fig. 4). Barrett overflowed more frequently and for lower runoff values than did Rodriguez. Barrett had zero overflow from 2006 to 2019 (R. Morales, personal communication), so we assume that Rodriguez also did not overflow in any year after 2010.

Annual Q correlated linearly with annual P in log-log space (Fig. 5). Four years with overflow (1980, 1983, 1993, 1995) had significantly more runoff than predicted using Eq. 3 (Fig. 5), suggesting either that the upper watershed produced large volumes of runoff in those years, or that there were non-linearities in the Q-P relationship in the lower watershed that are not captured by the log-linear function (Eq. 3). Changes in the Q-P relationship are discussed in Section 4.7.1.

4.6. Annual SSL, 1962–2019: Frequency analysis and assumptions about dams

Applying the bootstrapped parameters of Eq. 2 to the Q_{ann} time series from 1962 to 2019 generated 1000 values of SSL_{ann} for each year, from which we calculated a mean and standard deviation for each year (Fig. 6). The long-term mean SSL_{ann} was 0.128 ± 0.165 $Mt\ yr^{-1}$, with a range of 0.0012 – 0.574 $Mt\ yr^{-1}$. The coefficient of variation (CV = standard deviation / mean) of the bootstrapped values of SSL_{ann} was highest (30 %) for years with high rainfall.

Nearly half (46 %) of the cumulative SSL_{ann} over 1962–2019 occurred during very wet years (recurrence interval (Tr) ≥ 10 years); the wettest years ($Tr \geq 20$ years) contributed 28 % (Fig. 7) when using Q_{ann_lower} to predict SSL_{ann} . Slightly more than half of

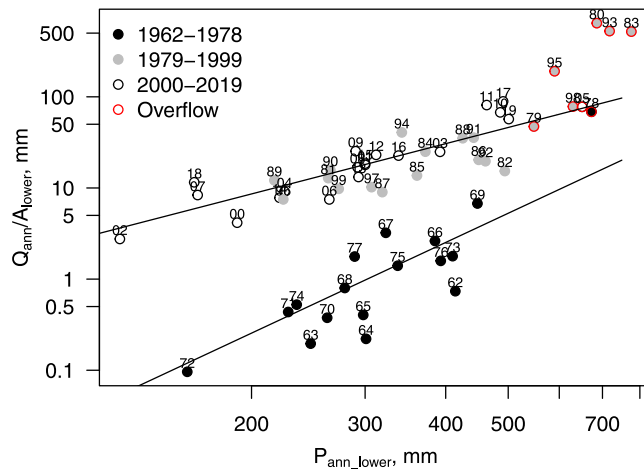


Fig. 5. Annual Q-P relationship for the Tijuana River. Text next to the points indicates the water year (e.g. 62 indicates 1962, 03 indicates 2003). The lower regression line is for pre-channelization and the upper line is for post-channelization, excluding years with overflow. Q_{ann} is the observed discharge.

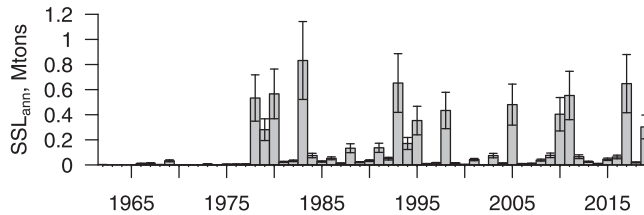


Fig. 6. Time series of annual suspended sediment load (SSL_{ann}) of the Tijuana River from 1962 to 2019, calculated using the annual SSL-Q relationship (Eq. 2 for 1979–2019; Brownlie and Taylor 1981 for 1962–1978) and Q_{ann_lower} as the predictor. Whiskers indicate one standard deviation, calculated using bootstrapping. SSL is non-zero for all years including 1962–1977.

the long-term SSL was contributed by years with a return interval of less than 10 years. A small fraction of SSL (5 %) was contributed by annual runoff with a Tr of 2-years or less.

Calculations of SSL_{ann} for years with dam overflow were highly sensitive to the Q values used in Eq. 2 and the corresponding

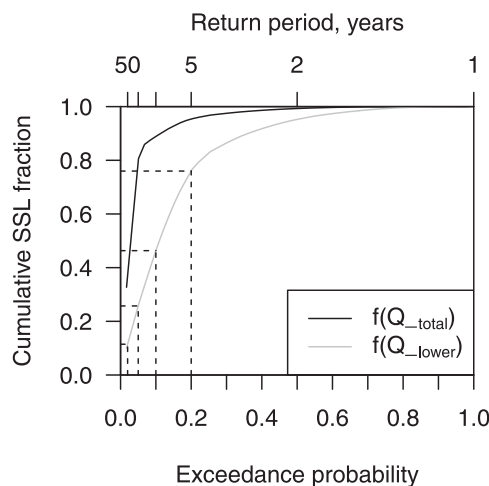


Fig. 7. Cumulative SSL_{ann} as a fraction of the total over 1962–2019 versus the exceedance probability and return period using either annual runoff from the total watershed area (Q_{ann_total}) (black line) or the lower watershed (Q_{ann_lower} , green line) to calculate SSL_{ann} . Both estimates use the same annual SSL-Q relationship (Eq. 2). Dashed lines indicate return periods of 5, 10, 20, and 50 years. The cumulative SSL over the whole period (1962–2019) was 23.9 Mt when using Q_{ann_total} and 4.9 Mt when using Q_{ann_lower} to estimate SSL_{ann} .

assumptions about dam impacts on SSL (Table 1). Using $Q_{\text{ann_total}}$ to predict SSL_{ann} , which assumes that dams do not impact the SSL-Q relationship, results in a much larger (7.1x) total SSL (0.920 Mt y^{-1}) over 1962–2019 compared with using $Q_{\text{ann_lower}}$ (0.128 Mt y^{-1}), which assumes complete retention by dams. Using $Q_{\text{ann_total}}$ also results in a larger contribution ($\sim 90\%$) of the wettest years ($Tr \geq 10$ years) to cumulative SSL_{ann} compared with using $Q_{\text{ann_lower}}$ (46% from the wettest years) (Fig. 7). The ratio of SSL estimated by using $Q_{\text{ann_total}}$ to SSL estimated using $Q_{\text{ann_lower}}$ ranged from 6.8 to 33.9 for the four wettest years (Table 1). The lower estimate, where SSL for years with overflow is calculated using $Q_{\text{ann_lower}}$, is likely more reliable, since dams typically retain a large percentage of the sediment load into them (85% for reservoirs in California, Willis and Griggs, 2003). Our purpose here is to quantify the range of possible SSL values and to demonstrate how not taking dams into account can bias SSL calculations in years with overflow.

4.7. Change over time

4.7.1. Changes in annual Q-P relationships and Q

Annual runoff (Q_{ann}) increased for a given annual rainfall after 1978, coinciding with the start of imported water and channelization, with the largest percentage increases at low annual rainfall (Fig. 5). The parameters of the Q-P relationship in the pre-1978 condition (1962–1978) were: bcf 1.24, g 5.1×10^{-9} , and h 3.305 ($R^2 = 0.62$); in the post-1978 condition the parameters were: bcf 1.10, g 4.7×10^{-4} , h 1.832 ($R^2 = 0.67$). The intercepts and slopes of the Q-P relationship were statistically different ($p < 0.01$) pre- and post-1978. Using the pre-1978 Q-P parameters to predict Q in the post-1978 period, years with no overflow only, gives mean annual runoff of 1.8 MCM, compared with 26.5 MCM observed, an approximate 15-fold increase. The mechanisms that could account for this increase are discussed in Section 5.2.

4.7.2. Changes in SSL-Q relationships

Annual SSL was higher for a given annual runoff in the 1970 s (BT81) compared to the 2000 s, except for the wettest years (Fig. 3). Additional SSC data from the USGS (1976–1978) not included in BT81 or IJ99 (Fig. 8, Fig. S21) suggests that SSL and SSC were consistently higher in the 1970 s than in 2019–2021 at low runoff ($0.1\text{--}1 \text{ m}^3 \text{ s}^{-1}$) but were highly variable for runoff greater than $1 \text{ m}^3 \text{ s}^{-1}$. Daily SSL in April, May and June (AMJ) 1978, for example, was significantly lower than daily SSL in 2019–2021, but SSL in AMJ was not different from other months for all other years in the 1970–1977 period (Fig. 8). Seasonality could account for the low SSC at high flows in 1978 AMJ, since AMJ is at the end of the wet season, but the available data do not allow for robust conclusions. All samples from the 1970 s were collected prior to channelization and imported water, which could have either increased or decreased SSC for a given runoff depending on the role of the channel and wastewater in providing sediment at low flows. Additional sampling may help quantify seasonal differences in the SSC-Q relationship and allow for a more robust comparison with historical data, though the lack of historical SSC data at high runoff complicates quantification of changes over time.

4.7.3. Changes in SSL-P relationships and annual SSL

Post-1978 SSL was several times higher than pre-1978 SSL for a given $P_{\text{ann_lower}}$ (Fig. 9). This suggests that higher SSC in the 1970 s was more than balanced by higher runoff production in the post-1978 period, resulting in higher SSL for a given annual P in the post-1978 period, with decreasing differences in wetter years. The slopes and intercepts of the SSL-P relationship were statistically significantly different pre- and post-1978 ($p < 0.05$). If the low SSC and SSL values observed in April and May of 1978 (Fig. 8) are more

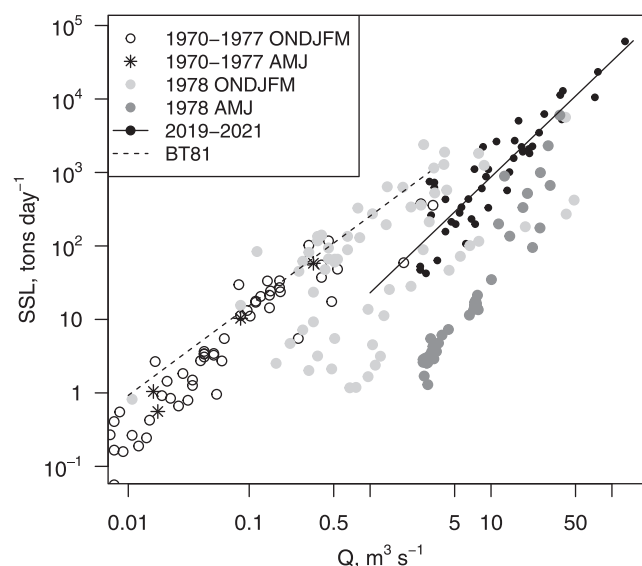


Fig. 8. Instantaneous sediment rating curves for 2019–2021 and comparison with data from the USGS (1970–1978) separated by season (Oct-Nov-Dec-Jan-Feb-Mar (ONDJFM) and Apr-May-June (AMJ)), and with the Brownlie and Taylor (1981) rating curves for the Tijuana River (BT81).

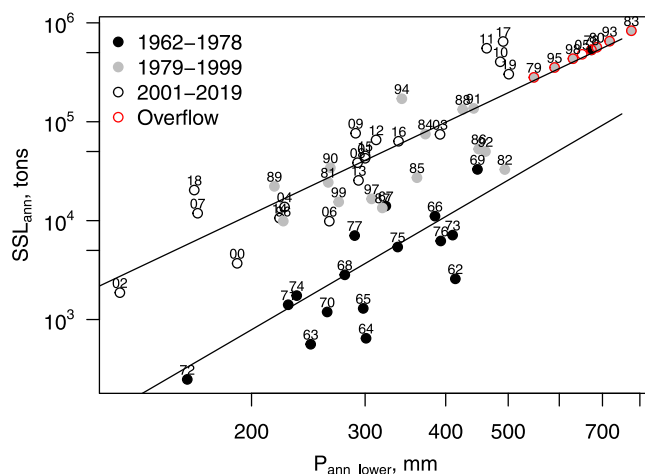


Fig. 9. Annual rainfall in the lower watershed ($P_{ann,lower}$) versus annual suspended sediment load (SSL_{ann}), by water year. Text next to the points indicate the water year (e.g. 62 indicates 1962, 03 indicates 2003). SSL for years with overflow is predicted from $Q_{ann,lower}$ estimated from the Q-P relationship for the lower watershed (Eq. 3).

representative than the higher values in 1970–1977, then the pre-1978 SSL would be even lower than our estimate.

SSL_{ann} during the post-1978 period (no overflow years only) calculated assuming pre-1978 parameter values (Eq. 4) was 7831 tons y^{-1} , while the mean for the same time period using the post-1978 parameter values was 94,888 tons y^{-1} . Combined, the increase in runoff (15-fold) more than compensated for any potential decrease in SSC, resulting in a 12-fold increase in SSL from pre- to post-1978 conditions. The impact of uncertainties in the historical and recent data, and the plausibility of this magnitude of change will be discussed in Section 5.2.

4.8. Comparison with other studies on the Tijuana River

Our upper-bound estimate of SSL during the wet period of IJ99 (1969–1995), using $Q_{ann,total}$ to predict SSL (1.85 Mtons yr^{-1}), was 5.3 times higher than the IJ99 estimate, while our lower-bound estimate using $Q_{ann,lower}$ (0.148 Mtons yr^{-1}) was 58 % lower than the IJ99 estimate (Table 2). Our higher SSL_{ann} estimate when using $Q_{ann,total}$ is due to our annual SSL-Q relationship (Fig. 5), which has higher SSL at high runoff ($Q_{ann} > 60$ MCM) than the relationship used by IJ99. Our SSL estimate using $Q_{ann,lower}$ is lower than IJ99 due to our assumption of reservoir retention of sediment during years of overflow, which dominate the long-term average. Due to the likelihood of high rates of sediment retention in the reservoirs and our additional SSC observations at high runoff, we believe that our revised estimate of 0.148 Mtons yr^{-1} over 1969–1995 is the most reliable, and that IJ99 may overestimate SSL. Not controlling for the

Table 2

Suspended sediment yield (SSY) for the Tijuana River and other watersheds draining similar geology (peninsular ranges) in southern California.

Watershed	SSY (tons $km^{-2} yr^{-1}$)	Reference
Other watersheds, peninsular ranges		
San Diego Creek	350	IJ99
San Juan Creek	170	IJ99
Santa Margarita	50	IJ99
San Luis Rey	300	IJ99
San Diego River	10	IJ99
Sweetwater	36	IJ99
Mean peninsular ranges	100	IJ99
Tijuana River ^a		
Pre-dam conditions	293 ^b	Inman and Masters (1991) Table 9–7
Post-dam conditions	74 ^b	Inman and Masters (1991) Table 9–7
Post-dam (1937–1975)	129	BT81 Table C10-5
Post-dam	131	Warrick and Farnsworth (2009)
Post-dam (1944–1995)	188	IJ99
Post-dam wet period (1969–1995)	315	IJ99
Post-dam wet period (1969–1995)	130	This study
Post dam all years (1962–2019)	119	This study
Los Laureles Canyon	5000	Biggs et al. (2018)

^a Yields calculated as total load divided by the active, undammed drainage only (A_{lower}).

^b Volumes converted to mass using bulk density of 1.67 tons m^{-3} . Yield in Inman and Masters (1991) is for sand and gravel.

time period, our estimated mean annual SSY over 1962–2019 is 38 % lower than IJ99 (years 1944–1995), and 15 % lower than the Warrick and Farnsworth (2009) estimates for the Tijuana River (Table 2).

5. Discussion

5.1. Dam impacts on SSL calculations

Assumptions about dams and their impact on the Q-SSL relationship had a large impact on SSL estimates, both for the years with overflow and for the long-term mean. Use of runoff from the lower watershed only ($Q_{\text{ann,lower}}$) to estimate suspended sediment loads (SSL_{ann}), which assumes complete retention of sediment behind dams, results in significantly lower SSL values compared with the use of $Q_{\text{ann,total}}$ (Table 1) and compared to previous estimates (IJ99). It also reduces the importance of the wettest years, which have much higher runoff (Fig. 4) but not significantly higher SSL (Fig. 6) due to retention of sediment behind the dams. This conclusion depends on accurate estimation of $Q_{\text{ann,lower}}$; non-linearities in the Q-P response could result in inaccurate estimates of $Q_{\text{ann,lower}}$, especially for years with high rainfall. Future research could use more detailed Q-P modeling of the lower watershed.

Our documentation of dam impacts on SSL estimates is important for estimates of SSL in other river basins with dams. Samples of SSC are often collected for relatively small, frequent storms when dam overflow may be unlikely; extrapolation of the SSL-Q relationship for years with overflow would then overestimate SSL. A systematic review of existing SSL estimates (e.g. IJ99) and sensitivity analysis using the method proposed here would help determine the magnitude of this potential overestimation.

5.2. Change over time

5.2.1. Annual runoff

Mean annual runoff increased by 24.7 MCM (15x) after 1978, controlling for precipitation variability. The increase in Q could be due to channelization of the Tijuana River in 1979 and to the start of importing of water from the Colorado River (1978). Channelization reduces channel infiltration, and could have reduced groundwater flow down the valley and reduced evapotranspiration from riparian vegetation. Limited data are available to determine the extent of the pre-1978 riparian vegetation, but riparian evapotranspiration (ET) can be approximated to a first-order: assuming riparian vegetation width ranging from 100 m to 500 m along the 4 km of channelized river, and 1260 mm per year of ET, equal to potential ET of the coastal region (Hart et al., 2009), gives annual ET of the pre-channel riparian zone of 2.5–3.8 MCM, which is much smaller than the change in annual runoff (24.7 MCM). Infiltration in the channel and floodplain with resulting down-valley groundwater flow may have further reduced surface flow before channelization, but estimation of this flow is beyond the scope of this paper. The volume of water imported from the Colorado River was 101.3 MCM by 2008 (Cohen et al., 2011), which is larger than the observed increase in runoff. Wastewater from Tijuana discharged directly to the river until 1997 when the International Water Treatment Plant was finalized. Further research is needed, including on how wastewater effluent, dams, channelization and urbanization affect the Q-P relationship, baseflow, stormflow, and annual Q.

5.2.2. Sediment rating curves and SSL

Annual (Fig. 5) and instantaneous sediment rating curves (Q vs SSL or SSC) (Fig. 8, Fig. S20) suggest that SSL for a given runoff was lower in 2001–2019 than in the 1970 s for low annual runoff but similar for higher runoff. There is considerable uncertainty in SSC for high flows as most of the 1970 s samples were collected at low flow ($<3.28 \text{ m}^3 \text{ s}^{-1}$). Instantaneous SSL was approximately 10x higher in 1970 s compared with 2019–2021 for low runoff (Fig. 8), except for April-June 1978, which had lower annual SSL for a given annual Q. Higher runoff post-1978 resulted in higher SSL despite the lower SSL for a given discharge. Our analysis suggests that SSL was 12x higher in the post-1978 condition than it would have been under pre-1978 conditions, assuming the sediment rating curves were stable for the full range of runoff observed. However, SSL in the post-dam period was still ~60% lower than SSL estimated for pre-dam conditions by Inman and Masters (1991), suggesting that SSL increased post-1978 compared with 1962-1978 conditions, but likely not to pre-dam levels (Table 2).

5.3. Land use and channelization impacts on SSL

Sediment management in Tijuana, especially the installation of sedimentation basins, may have reduced the sediment load under conditions of low runoff; large human impacts on small runoff events, with limited impacts on large events, is also seen in floods, where land use has the biggest impact for return periods of < 5 years (White and Greer 2006). In addition, impervious cover is high (50–80 %) in the urban core of Tijuana (Biggs et al., 2010), and many stream channels have been lined with concrete, both of which could reduce SSL below the pre-urban background (Wolman, 1967). More work is needed to calculate the historical and contemporary rating curves and SSL of the Tijuana River and how they are impacted by seasonality, management, and land cover change.

5.4. Comparisons with other watersheds in southern California

SSL for watersheds in the peninsular ranges of southern California averaged $100 \text{ tons km}^{-2} \text{ yr}^{-1}$ and ranged from 10 to 350 $\text{tons km}^{-2} \text{ yr}^{-1}$ (IJ99). Tijuana River SSL from our study (Table 2) is within the range of other watersheds in the peninsular range, suggesting that, while urbanization may have increased SSL above the pre-urban baseline, urbanization does not appear to have increased the SSL of the Tijuana River beyond the range observed in other watersheds in southern California. However, channelization and

imported water coincided with a large increase in runoff for a given annual rainfall (Fig. 4), and year was a significant predictor of annual runoff after controlling for annual rainfall; combined this resulted in a ~12-fold increase in SSL compared with pre-1978 conditions. However, dam construction has likely reduced sediment load by 50–75 % from pre-dam conditions (Table 2) (IJ99, Inman and Masters, 1991). Significant uncertainty remains about the combined impacts of dam construction, imported water, urbanization and channelization on runoff and sediment loads.

In contrast with the Tijuana River and other peninsular ranges, SSY in the Los Laureles Canyon watershed (LLCW) (~11.6 km²), which drains directly into the Tijuana Estuary, was extremely high (5000 tons km⁻² y⁻¹; Biggs et al., 2018) and roughly 42 times the SSY of the Tijuana River. The trap data used for the LLCW includes bedload, but the trapped sediment was only approximately 10–15 % by weight cobbles or larger (>64 mm diameter), and most of the sediment in the trap is fine to very fine sand (Taniguchi, unpublished data). The undammed side canyons draining to the Tijuana Estuary have much higher sediment yields than the mainstem of the Tijuana River, with consequent high sedimentation rates and impacts on the southern part of the estuary.

5.5. Implications for sediment accumulation and management

Our results suggest a paradox: runoff and annual suspended sediment load from the Tijuana River has likely increased during urbanization, but loads in the post-dam period (1936-present) are likely still lower than the pre-dam load (Table 2), and yet the Tijuana Estuary has lost most of its tidal prism due to high rates of sediment accumulation (Safran et al., 2017). The Tijuana River also does not have significantly higher loads than other streams on similar lithology. The paradox could be explained in part by the reduction in stormflow and consequent reduced transport capacity of the river following dam construction: BT81 estimate that annual flow in the Tijuana River decreased from 8.6 MCM in pre-dam conditions to 1.6 MCM in the post-dam but pre-channelization period (1951–1975), a reduction of 81 % (Table C11–3 in BT81). Annual and peak runoff increased following channelization and urbanization in the post-dam period (Fig. 5), though it is unclear whether flows reached their pre-dam levels. Significant uncertainty remains about the magnitudes of pre-dam runoff and SSL, and the runoff necessary to transport sediment through the estuary to the coast.

6. Conclusion

6.1. Main findings

Flood events larger than the 2-year recurrence interval (N = 10) accounted for more than half of total suspended sediment load (SSL) of the Tijuana River over 2001–2019, but frequent floods smaller than the 2-year event also accounted for nearly half of SSL. Over the longer time period (1962–2019), the 10 % wettest years accounted for 48 % of SSL, while the driest 50 % of years accounted for less than 5 %. Extreme events may have less impact on decadal cumulative SSL than previously documented (IJ99), due to the impact of sediment retention by dams on SSL estimates during years with dam overflow. Overall, large events and wet years are important for the long-term load, but more frequently occurring years and events are also important.

SSL in the Tijuana River likely decreased from 1970 s to 2019–2021 for small storms due to higher suspended sediment concentrations in the 1970 s, but annual runoff increased markedly, resulting in a net increase in annual SSL. The SSL from the Tijuana River is still likely around half of the load prior to construction of dams upstream (IJ99, Inman and Masters, 1991), and delivery of sediment to the coast is likely further reduced by a reduction in flow and transport capacity (Willis and Griggs, 2003). Reduced flow in the post-dam period likely contributes to accumulation of sediment in the Tijuana estuary, and to low sediment loads to the ocean and consequent beach erosion.

6.2. Limitations and future work

Sediment load estimates are uncertain, especially during the wet years (Tr > 10 y) that account for approximately half of the total SSL. Our calculations of SSL and the impact of dams depend on accurate estimation of runoff from the lower watershed, and stability of the annual SSL-Q relationship. The abrupt increase in runoff post-1978 coincides with channelization and the start of imported water, but changes in measured runoff could also be caused in part by changes in the methods, equipment or rating curves associated with channelization. Q-P and SSL-Q relationships may change markedly during extreme events, but the current dataset, and most similar datasets, do not have SSC data for those events. Future work could model annual runoff and sediment loads for upper and lower watersheds in the few extreme wet years, including the trapping efficiencies of the two main reservoirs. Sediment loads may have increased post-channelization and post-urbanization due to increased runoff, but significant uncertainty in the historical (1960–70 s) relationship between runoff and SSL precludes precise estimates.

Our analysis quantifies changes in runoff and sediment loading over time, but does not identify the mechanism responsible for the changes. Channelization, urban wastewater, impervious surface, soil exposure, and channel erosion could all contribute to changes in runoff and/or sediment loads. Future work could model runoff and sediment loads and analyze intra-annual changes in flow duration curves to identify mechanisms responsible for the observed changes.

Both drought and flood frequency are projected to increase in the region (Ashraf Vaghefi et al., 2017; Modrick and Georgakakos, 2015). SSL is a non-linear function of rainfall, so increases in both wet and dry years could cause a net increase in SSL to the estuary, even if long-term mean rainfall does not change. The interacting effects of climate variability, channelization, urbanization, imported water, runoff, sediment loads, estuarine sedimentation rates and ecosystem impacts require further quantification.

6.3. Implications and broader impacts

Our methods and findings have implications for calculations of sediment loads in other locations. First, event-wise modeling of sediment loads can leverage municipal monitoring datasets, which may be event-wise composites and not instantaneous values used in traditional rating curve construction. Second, the relationships between annual rainfall, runoff and sediment loads can be highly impacted by dams upstream, especially during extreme wet years when dams overflow, but this is often difficult to quantify due to limited data availability for extreme events. Sediment retention behind dams can reduce sediment concentrations downstream, but such effects may not be included in sediment rating curves fit to SSC measurements taken at low runoff without dam overflow. Uncertainty analysis as performed here can help quantify possible dam impacts on calculations of long-term sediment loads. Third, we quantify uncertainty in the sediment-runoff relationships using bootstrapping and provide an updated estimation of long-term sediment loads and trends, which can be used to inform future sediment management and restoration efforts. Revised sediment-runoff relationships can also be used to calibrate watershed models to evaluate the effects of sea level rise, climate change, and land use changes on future sediment loads and resilience of coastal wetlands.

Funding

This work was supported by the State of California - The Natural Resources Agency, California Ocean Protection Council, USA [Agreement # C0304100] under the Safe Drinking Water, Water Quality and Supply, Flood Control, River and Coastal Protection Bond Act of 2006 – Proposition 84. T.B. was supported in part by the United States Environmental Protection Agency, Regional Applied Research Effort Program [Agreement # 68HE0B21P0637].

CRedit authorship contribution statement

T.B. led manuscript preparation, prepared figures and tables and analyzed data. A.Z. led fieldwork, analyzed samples, prepared databases, analyzed data, and drafted sections of the paper. K.T. procured funds for fieldwork, coordinated field data collection and installations, prepared figures, analyzed data, and helped draft and edit the text.

Declaration of Competing Interest

The authors declare the following financial interests/personal relationships which may be considered as potential competing interests: Trent Biggs reports financial support was provided by the United States Environmental Protection Agency, Regional Applied Research Effort Program. Kris Taniguchi reports financial support was provided by State of California - The Natural Resources Agency, California Ocean Protection Council. Adam Zeigler reports financial support was provided by State of California - The Natural Resources Agency, California Ocean Protection Council.

Acknowledgements

Bryn Evans (Dudek consulting) identified and provided the TSS data for 2002–2013. Ben Downing, Liesl Tiefenthaler, Dario Diehl, John Murphy and Jordan Ferreira assisted with the autosampler and laboratory analysis. Rosalva Morales and Quinn Alkin of the City of San Diego provided reservoir spillway data. Doug Liden (US EPA) and Eric Stein (SCCWRP) provided comments on drafts of the manuscript.

Supplemental Materials

Supplementary data associated with this article can be found in the online version at [doi:10.1016/j.ejrh.2022.101162](https://doi.org/10.1016/j.ejrh.2022.101162).

References

- Acosta, J.Á.E., 2009. Migration and urbanization in Northwest Mexico's border cities. *J. Southwest* 51, 445–455 <https://doi.org/http://www.jstor.org/stable/40599702>.
- Ashraf Vaghefi, S., Abbaspour, N., Kamali, B., Abbaspour, K.C., 2017. A toolkit for climate change analysis and pattern recognition for extreme weather conditions – Case study: California-Baja California Peninsula. *Environ. Model. Softw.* 96, 181–198. <https://doi.org/10.1016/j.envsoft.2017.06.033>.
- Biggs, T.W., Atkinson, E., Powell, R., Ojeda-Revah, L., 2010. Land cover following rapid urbanization on the US–Mexico border: implications for conceptual models of urban watershed processes. *Landsc. Urban Plan.* 96, 78–87. <https://doi.org/10.1016/j.landurbplan.2010.02.005>.
- Biggs, T.W., Taniguchi, K.T., Gudino-Elizondo, N., Langendoen, E.J., Yuan, Y., Bingner, R.L., Liden, D., 2018. Runoff and sediment yield on the US-Mexico border, Los Laureles Canyon, EPA/600/R-18/365. Washington, D.C.
- Brown, R.G., 1988. Effects of wetland channelization on runoff and loading. *Wetlands* 8, 123–133. <https://doi.org/10.1007/BF03160597>.
- Brownlie, W.R., Taylor, B.D., 1981. Sediment management for southern California mountains, coastal plains and shoreline. Part C: Coastal sediment delivery by major rivers in southern California, EQL Report No. California Institute of Technology, Pasadena, CA.
- Chapman, J.M., Proulx, C.L., Veilleux, M.A.N., Levert, C., Bliss, S., André, M.-È., Lapointe, N.W.R., Cooke, S.J., 2014. Clear as mud: a meta-analysis on the effects of sedimentation on freshwater fish and the effectiveness of sediment-control measures. *Water Res.* 56, 190–202. <https://doi.org/10.1016/j.watres.2014.02.047>.

- City of San Diego, 2021. Reservoirs and Lakes: Barrett Reservoir [WWW Document]. URL <https://www.sandiego.gov/reservoirs-lakes/barrett-reservoir> (accessed 12.17.21).
- Cohen, M.J., Martin, J.C., Ross, N., Luu, P., 2011. Municipal Deliveries of Colorado River Basin Water. Oakland, CA Pacific Inst.
- Crawford, C.G., 1991. Estimation of suspended-sediment rating curves and mean suspended-sediment loads. *J. Hydrol.* 129, 331–348. [https://doi.org/10.1016/0022-1694\(91\)90057-0](https://doi.org/10.1016/0022-1694(91)90057-0).
- Dedkov, A.P., Mozzherin, V.I., 1996. Erosion and sediment yield on the Earth. *IAHS Publ. Proc. Intern Assoc. Hydrol. Sci.* 236, 29–36.
- Duvert, C., Nord, G., Gratiot, N., Navratil, O., Nadal-Romero, E., Mathys, N., Némery, J., Regués, D., García-Ruiz, J.M., Gallart, F., Esteves, M., 2012. Towards prediction of suspended sediment yield from peak discharge in small erodible mountainous catchments (0.45–22km²) of France, Mexico and Spain. *J. Hydrol.* 454–455, 42–55. <https://doi.org/10.1016/j.jhydrol.2012.05.048>.
- Fennessey, L.A.J., Jarrett, A.R., 1994. The dirt in a hole: a review of sedimentation basins for urban areas and construction sites. *J. Soil Water Conserv.* 49, 317 LP–317323.
- Gudino-Elizondo, N., Biggs, T., Bingner, R., Yuan, Y., Langendoen, E., Taniguchi, K., Kretzschmar, T., Taguas, E., Liden, D., 2018. Modelling ephemeral gully erosion from unpaved urban roads: equifinality and Implications for Scenario analysis. *Geosciences* 8, 137. <https://doi.org/10.3390/geosciences8040137>.
- Fuka, D.R., Walter, M.T., Archibald, J.A., Steenhuis, T.S., Easton, Z.M. EcoHydrology: A Community Modeling Foundation for Eco-Hydrology. R package version 0.4.12.1. <https://CRAN.R-project.org/package=EcoHydrology>.
- Gray, J.R., Glysson, G.D., Turcios, L.M., Schwarz, G.E., 2000. Comparability of suspended-sediment concentration and total suspended solids data, Water-Resources Investigations Report 00-4191. U.S. Dept. of the Interior, U.S. Geological Survey, Reston, VA. <https://doi.org/10.3133/wri004191>.
- Gudino-Elizondo, N., Biggs, T.W., Bingner, R.L., Langendoen, E.J., Kretzschmar, T., Taguas, E.V., Taniguchi-Quan, K.T., Liden, D., Yuan, Y., 2019. Modelling runoff and sediment loads in a developing coastal watershed of the US-Mexico border. *Water* 11, 1024. <https://doi.org/10.3390/w11051024>.
- Hart, Q.J., Brugnach, M., Temesgen, B., Rueda, C., Ustin, S.L., Frame, K., 2009. Daily reference evapotranspiration for California using satellite imagery and weather station measurement interpolation. *Civ. Eng. Environ. Syst.* 26, 19–33. <https://doi.org/10.1080/10286600802003500>.
- Inman, D.L., Jenkins, S.A., 1999. Climate Change and the Episodicity of Sediment Flux of Small California Rivers. *J. Geol.* 107, 251–270. <https://doi.org/10.1086/314346>.
- Inman, D.L., Masters, P.M., 1991. Ch. 9. Budget of sediment and prediction of the future state of the coast, in: *Coast of California Storm and Tidal Waves Study*. United States Army Corps of Engineers, Los Angeles, CA.
- International Boundary and Water Commission, 2021. Tijuana River Flood Control Project (TRFCP) [WWW Document]. URL https://www.ibwc.gov/mission_operations/tj_river_fcp.html (accessed 5.23.22).
- International Boundary and Water Commission, 2005. Western Water Bulletin: Flow of the Colorado River and other Western Boundary Streams and Related Data.
- International Boundary and Water Commission, 1966. Western Water Bulletin: Flow of the Colorado River and other Western Boundary Streams and Related Data. Department of State.
- Li, T., Wang, S., Fu, B., Feng, X., 2020. Frequency analyses of peak discharge and suspended sediment concentration in the United States. *J. Soils Sediment.* 20, 1157–1168. <https://doi.org/10.1007/s11368-019-02463-8>.
- Manago, K.F., Hogue, T.S., 2017. Urban streamflow response to imported water and water conservation policies in Los Angeles, California. *JAWRA J. Am. Water Resour. Assoc.* 53, 626–640. <https://doi.org/10.1111/1752-1688.12515>.
- Mentaschi, L., Vousdoukas, M.I., Pekel, J.-F., Voukouvalas, E., Feyen, L., 2018. Global long-term observations of coastal erosion and accretion. *Sci. Rep.* 8, 12876. <https://doi.org/10.1038/s41598-018-30904-w>.
- Messina, A.M., Biggs, T.W., 2016. Contributions of human activities to suspended sediment yield during storm events from a small, steep, tropical watershed. *J. Hydrol.* 538, 726–742. <https://doi.org/10.1016/j.jhydrol.2016.03.053>.
- Modrick, T.M., Georgakakos, K.P., 2015. The character and causes of flash flood occurrence changes in mountainous small basins of Southern California under projected climatic change. *J. Hydrol. Reg. Stud.* 3, 312–336. <https://doi.org/10.1016/j.ejrh.2015.02.003>.
- Muñoz-Sabater, J., 2019. ERA5-land monthly averaged data from 1981 to present. Copernic. *Clim. Chang. Serv. Clim. Data Store* 10, 24381. <https://doi.org/10.24381/cds.68d2bb30>.
- Muñoz-Sabater, J., Dutra, E., Agustí-Panareda, A., Albergel, C., Arduini, G., Balsamo, G., Boussetta, S., Choulga, M., Harrigan, S., Hersbach, H., Martens, B., Miralles, D.G., Piles, M., Rodríguez-Fernández, N.J., Zsoter, E., Buontempo, C., Thépaut, J.-N., 2021. ERA5-Land: a state-of-the-art global reanalysis dataset for land applications. *Earth Syst. Sci. Data* 13, 4349–4383. <https://doi.org/10.5194/essd-13-4349-2021>.
- Rustomji, P., Wilkinson, S.N., 2008. Applying bootstrap resampling to quantify uncertainty in fluvial suspended sediment loads estimated using rating curves. *Water Resour. Res.* 44. <https://doi.org/10.1029/2007WR006088>.
- Safran, S., Baumgarten, S., Beller, E., Crooks, J., Grossinger, R., Lorda, J., Longcore, T., Bram, D., Dark, S., Stein, E., 2017. Tijuana river valley historical ecology investigation. San Francisco Estuary Institute-Aquatic Science Center, Richmond, CA.
- Simon, A., 1989. The discharge of sediment in channelized alluvial streams. *JAWRA J. Am. Water Resour. Assoc.* 25, 1177–1188. <https://doi.org/10.1111/j.1752-1688.1989.tb01330.x>.
- Slagel, M.J., Griggs, G.B., 2008. Cumulative losses of sand to the California coast by dam impoundment. *J. Coast. Res.* 243, 571–584. <https://doi.org/10.2112/06-0640.1>.
- Taniguchi, K.T., Biggs, T.W., Langendoen, E.J., Castillo, C., Gudino-Elizondo, N., Yuan, Y., Liden, D., 2018. Stream channel erosion in a rapidly urbanizing region of the US-Mexico border: documenting the importance of channel hardpoints with structure-from-motion photogrammetry. *Earth Surf. Process. Landf.* 43, 1465–1477. <https://doi.org/10.1002/esp.4331>.
- Tarolli, P., Sofia, G., 2016. Human topographic signatures and derived geomorphic processes across landscapes. *Geomorphology* 255, 140–161. <https://doi.org/10.1016/j.geomorph.2015.12.007>.
- URS Corporation, 2012a. Sediment yield estimate of the Tijuana River, DOC ID# CSD-RT-12-URS38.02.F. Prepared for City of San Diego, San Diego, CA.
- URS Corporation, 2012b. Analysis of extreme peak flows for the main Tijuana River, San Diego, California, DOC ID# CSD-TR-12-URS38.01.F. Prepared for City of San Diego, San Diego, CA.
- US Army Corps of Engineers, 2018. Phase I Hydrology, Floodplain and Sediment Transport Report Final – Tijuana River United States-Mexico International Border to the Pacific Ocean. Los Angeles, CA.
- Wallace, K.J., Callaway, J.C., Zedler, J.B., 2005. Evolution of tidal creek networks in a high sedimentation environment: A 5-year experiment at Tijuana Estuary, California. *Estuaries* 28, 795–811. <https://doi.org/10.1007/BF02696010>.
- Walling, D.E., 2012. The role of dams in the global sediment budget. *Eros. Sediment Yields Chang. Environ. IAHS Publ.* 356, 3–11.
- Warrick, J.A., Melack, J.M., Goodridge, B.M., 2015. Sediment yields from small, steep coastal watersheds of California. *J. Hydrol. Reg. Stud.* 4, 516–534. <https://doi.org/10.1016/j.ejrh.2015.08.004>.
- Weis, D.A., Callaway, J.C., Gersberg, R.M., 2001. Vertical accretion rates and heavy metal chronologies in Wetland sediments of the Tijuana Estuary. *Estuaries* 24, 840. <https://doi.org/10.2307/1353175>.
- Weston Solutions, 2015. Transitional receiving water monitoring work plan. Prepared for San Diego County Regional Copermitees, Carlsbad, CA.
- Willis, C.M., Griggs, G.B., 2003. Reductions in fluvial sediment discharge by Coastal Dams in California and implications for beach sustainability. *J. Geol.* 111, 167–182. <https://doi.org/10.1086/345922>.
- M.G. Wolman A Cycle of Sedimentation and Erosion in Urban River Channels. *Geogr. Ann. Ser. A Phys. Geogr.* 49 1967 385 395 doi: 10.1080/04353676.1967.11879766.
- Zedler, J.B., West, J.M., 2008. Declining diversity in natural and restored salt marshes: a 30-Year Study of Tijuana Estuary. *Restor. Ecol.* 16, 249–262. <https://doi.org/10.1111/j.1526-100X.2007.00268.x>.
- R Core Team, 2021. R: A language and environment for statistical computing. R Foundation for Statistical Computing, Vienna, Austria. URL <https://www.R-project.org/>.